Available online at www.sciencedirect.com
ScienceDirect
Journal of Photochemistry and Photobiology A: Chemistry 189 (2007) 153–160
Journal of Photochemistry and Photobiology A:Chemistry
www.elsevier.com/locate/jphotochem

Dye-sensitized solar cells based on TiO_2 nanotubes and a solid-state electrolyte

Ismael C. Flores [a], Jilian Nei de Freitas [a], Claudia Longo [a], Marco-Aurelio De Paoli [a], Herbert Winnischofer [b], Ana Flávia Nogueira [a,*]

[a] *Laboratório de Nanotecnologia e Energia Solar, LNES, Instituto de Química, UNICAMP, C. Postal 6154, 13084-971 Campinas, SP, Brazil*
[b] *Departamento de Química, Universidade Federal do Paraná, UFPR, 81531-990 Curitiba, PR, Brazil*

Received 11 December 2006; received in revised form 9 January 2007; accepted 20 January 2007
Available online 25 January 2007

Abstract

Anatase TiO_2 nanotubes were employed with success as photoanode in dye-sensitized solar cells (DSSC) using a plasticized polymer electrolyte based on a poly(ethylene oxide) derivative. The plasticized electrolyte, poly(ethylene oxide-co-epychlorohydrin) containing NaI–I_2 had their conductivity and thermal behavior characterized as a function of the salt content. The highest ionic conductivity (5.5×10^{-4} S cm^{-1}) was obtained with 12.5 wt% NaI and 50 wt% of the plasticizer poly(ethyleneglycol)dibenzoate. The TiO_2 nanotubes were prepared by a simple sol–gel route and were characterized by FEG-SEM, TEM, XRD and BET. For the same film thickness, the DSSC assembled with the titania nanotubes had much higher efficiency in comparison with the device using TiO_2 nanoparticles. Although the one-dimensional properties exhibited by these materials can improve the electronic transport, in this study we demonstrated that the increase in the DSSC performance may be much more closely related to the high surface area of the titania films. This more open structure allows much more dye to be chemically absorbed and also facilitates the penetration of the polymer electrolyte, improving the iodide diffusion inside the film. We also observed that it was necessary to introduce a film of nanoparticulated TiO_2 prior deposition of the nanotubes in order to improve electrical contact with the conducting glass. Devices with efficiency of 4.03% at 100 mW cm^{-2} (Xe(Hg) lamp) can be obtained using a combination of TiO_2 nanotubes and this plasticized polymer electrolyte.

Keywords: Dye-sensitized solar cells; Plasticized polymer electrolyte; Titania nanotubes

1. Introduction

Dye-sensitized solar cells (DSSC) based on nanocrystalline inorganic oxides such as TiO_2, ZnO and SnO_2 have attracted much attention since their first description in the beginning of the 1990s by Grätzel and O'Reagan [1]. DSSC are currently attracting extensive academic and industrial interest envisioning this technology as a powerful and promising way to generate electricity from the Sun at low cost and with high efficiency. Nowadays, overall efficiencies of 11% have been reported for DSSC using liquid electrolytes [2].

In DSSC, the nanoparticulated oxide layer is generally TiO_2 with a high surface area, sensitized with a charge transfer ruthenium polypyridine complex dye, which absorbs light in the visible range of the solar spectrum. Energy conversion is achieved by injection of electrons from the photoexcited state of the sensitizer dye into the conduction band of the nanocrystalline semiconductor. This process is very fast, occurring on a sub-picosecond time scale [3]. These cells also employ a liquid electrolyte, usually an iodide/tri-iodide redox couple dissolved in an organic solvent, to regenerate the dye cation produced after electron transfer. Regeneration of iodide ions, which are oxidized in this reaction to tri-iodide, is achieved at a platinum counter electrode.

The liquid electrolyte usually employed in DSSC is still a drawback for long-term practical operation and causes substantial problems in bringing DSSC onto market. To overcome these problems, many research groups have been searching for alternatives to replace the liquid electrolytes, such as inorganic or organic hole conductors [4,5], ionic liquids [6–8], polymer [9–11] and gel electrolytes [12–15].

Since 1999, our group has been working on DSSC using polymer electrolytes based on poly(ethylene oxide) copolymers as an alternative to liquid electrolytes [16]. The best solar energy

* Corresponding author. Tel.: +55 19 3521 3029; fax: +55 19 3521 3023.
E-mail address: anaflavia@iqm.unicamp.br (A.F. Nogueira).

1010-6030/$ – see front matter © 2007 Elsevier B.V. All rights reserved.
doi:10.1016/j.jphotochem.2007.01.023

conversion efficiency obtained for a solid-state DSSC (1 cm^2 of active area) was 2.6% under 10 mW cm^{-2} and 1.6% under 100 mW cm^{-2} [9]. These efficiencies are too low for practical applications. Besides, our knowledge of polymer science suggests that the limit for DSSC efficiency, based on a system containing only polymer and salt as components, cannot exceed 3%. Modifications in the polymer/salt medium that can bring improvements to the ionic conductivity (e.g. addition of plasticizers or inorganic nanoparticles, gel electrolytes) and modifications in the structure of the TiO_2 electrodes must be pursued in order to develop DSSC with higher efficiencies. It is well established that the cell's performance is directly related to the ionic conductivity of the polymer electrolyte, which is a consequence of the iodide/tri-iodide mobility in the polymer matrix, and to electron transport through the oxide layer where vectorial transport achieved in a one-dimensional structure can help to minimize recombination losses during electronic transport.

TiO_2 nanoparticle films have been used as the photoelectrode in DSSC because of its high specific surface area that allows the adsorption of a large number of dye molecules. These nanoparticles have been prepared by several synthetic routes in a variety of particle sizes, pore size distributions and crystallinities. These factors affect the electron transport and as consequence, the charge recombination kinetics and the dark current of these cells. Besides, the electron diffusion coefficient determined by laser flash-induced transient photocurrent measurement [17,18] and intensity-modulated photocurrent spectroscopy for TiO_2 nanoparticles [19,20] was more than two orders of magnitude lower than for bulk anatase. The decrease in the electron diffusion coefficient can be a consequence of the presence of electron traps that occur in the grain boundaries at the contacts between the nanoparticles. Thus, the use of oxide semiconductors in the form of nanorods, nanowires and nanotubes may be an interesting approach to improve electron transport through the film. Due to the one-dimensional nature of these nanostructures, their morphology facilitates the electron transfer up to the collecting electrode, decreasing the ohmic loss through the TiO_2 nanorod. Besides, a high level of dye adsorption on the TiO_2 nanorod is expected due to the high surface area presented in these nanostructures [21,22]. Several groups have obtained promising and interesting results using these nanostructures as electrodes in photoelectrochemical and photovoltaic devices [21–30]. Uchida et al. were the first to report the application of TiO_2 nanotubes in DSSC with efficiency of 3.0% [31]. Adachi and co-workers have done a successful investigation about the introduction of TiO_2 nanowires [21] and nanorods [22] as photoanodes in these cells, achieving efficiencies of 9.0%. The increase in the DSSC's conversion efficiency has been assigned to an enhancement in the charge percolation pathway and high absorption of the ruthenium dye. More recently, Grimes and co-workers [32] described the use of highly ordered transparent TiO_2 nanotube arrays in DSSC with an efficiency of 2.9% for a 360 nm thick array (*viz.* the thickness of the nanoparticulated films usually employed is approximately 10 μm). The strategy of creating an organized axial arrangement of the nanotubes promotes an improvement in the charge separation and charge transport in these solar cell devices.

In this paper we demonstrated that a solid-state DSSC with improved efficiency can be easily accomplished using a combination of TiO_2 nanotubes and a plasticized polymer electrolyte. Our results show that adding a plasticizer in the polymer matrix improves the ionic conductivity of the electrolyte by one order of magnitude. Besides, the introduction of TiO_2 nanotubes, with a much more open structure, allows that the polymer electrolyte penetrates easily inside the film, increasing the interfacial contact between the nanotubes/dye and the electrolyte. In the other hand, the high surface area of TiO_2 nanotubes also allows more sensitizer dyes to be chemically attached to the semiconductor surface. As a consequence the device's performance at a light intensity of 100 mW cm^{-2} (Xe(Hg) lamp) is drastically improved, reaching 4.03%, in comparison with the same device using TiO_2 nanoparticles. We do not discard the influence of these one-dimensional electrodes in the electron transport, in our work, however, the use of these nanostructures seems to have a much higher effect on the semiconductor–electrolyte interface, creating an ample ion path for the iodide/tri-iodide diffusion and also on the increased amount of ruthenium dye adsorbed. From our knowledge, this is the first report of a solid-state DSSC combining a polymer electrolyte and titania nanotubes.

2. Experimental

2.1. TiO_2 nanotube synthesis

There are several reports in the literature on the synthesis of TiO_2 nanotubes, nanorods and nanowires using sol–gel, electrodeposition and hydrothermal methods [33–38]. In this work, anatase TiO_2 nanotubes were prepared following the first experimental report of these nanostructures by Kasuga et al. [34]. The choice for this method is due to its reproducibility and simplicity. Several groups have already reported DSSC made of nanotubes/nanowires synthesized by this method using liquid electrolytes [31,39,40]. Although in the method reported by Kasuga, they have concluded that the silica precursor added to the sol–gel mixture plays no role in the formation of the TiO_2 nanotubes, we choose to add this precursor, since no information has been reported that could guarantee that the size and distribution of the nanotubes would not be vary in the absence of this reagent. The procedure starts with the addition of 23.5 mL of titanium isopropoxide ($Ti(O\textit{i}\text{-}C_3H_7)_4$, from Acros Organics) and 4.5 mL of tetraethoxysilane ($Si(OEt)_4$, from Aldrich) in 23 mL of ethanol. The resulting solution was stirred for 15 min at room temperature. In a separated container, 18 g of 4.4 mol L^{-1} HCl in distilled water were added to 23 mL of ethanol. This solution was then slowly added to the mixture of $Ti(O\textit{i}\text{-}C_3H_7)_4$ and $Si(OEt)_4$ in ethanol. The mixture was allowed to hydrolyze and gel for 3 days at 40 °C and 70% relative humidity. The gel obtained was then heated to 600 °C and held for 2 h, resulting in the precipitation of fine TiO_2 crystals. Amorphous SiO_2-related phases are also present. Part of this gel was treated with a 10 mol L^{-1} NaOH solution for 48 h at 110 °C in an autoclave. Afterwards, the product was washed with distilled water and neutralized with an aqueous 0.1 mol L^{-1} HCl solu-

tion. The treated powders were then separated from the mixture by centrifugation and washed with distilled water several times until pH ∼ 7. The solid was dried at 90 °C for 3 h followed by calcination at 450 °C for 30 min. This calcination step guarantees the formation of anatase TiO_2 nanotubes as evidenced by XRD.

2.2. TiO_2 nanotube characterization

Structural characterization of the TiO_2 nanotubes were done by X-ray diffraction (XRD) using a Shimadzu XRD 7000 with Cu Kα radiation, λ = 0.154 nm, transmission electron microscopy (TEM) with a Jeol JEM-3010 operating at 300 kV and scanning electron microscopy (FEG-SEM) with a Jeol JSM 6330F. Nitrogen adsorption isotherms were obtained with a Micromeritics FlowSorb II 2300 equipment. To evaluate the properties of the TiO_2 nanotubes in DSSC, a titania suspension containing 1.0 g of TiO_2 nanotubes and 0.3 g of polyethylene glycol (PEG 20000) in 3 mL of distilled water was spread onto a conducting glass substrate with a glass rod. The film was then heated at 450 °C for 30 min to ensure electrical contact between the nanotubes and the conducting substrate. Film thickness was recorded by an Alpha Step 200 Tencor Instrument.

2.3. Polymer electrolyte preparation

Samples of the copolymer poly(ethylene oxide-co-epichlorohydrin) were used as received from Daiso Co. Ltd. (Osaka). The ethylene oxide/epichlorohydrin ratio in the copolymer was 84/16 and is designated as P(EO-EPI)84:16. The copolymer molar mass reported by the supplier was *ca.* 1×10^6 g mol^{-1}. The polymer electrolyte solution was prepared by co-dissolution of the copolymer, NaI, I_2 and the plasticizer poly(ethyleneglycol)dibenzoate (PEG-diB, Aldrich) in acetone. The choice of PEG-diB as plasticizer was based on its low molar mass, high boiling point and chemical similarity to the poly(ethylene oxide-co-epichlorohydrin) copolymer. The chemical compatibility is important to promote better diffusion of the plasticizer molecules through polymer chains. The copolymer/plasticizer weight ratio was 1:1.

2.4. Polymer electrolyte characterization

Polymer electrolyte samples with different salt contents were prepared according to the procedure described above. The plasticized polymer electrolyte ionic conductivity was analyzed by electrochemical impedance spectroscopy (EIS). The thermal behavior was characterized by differential scanning calorimetry (DSC) and thermogravimetric analysis (TGA) (see Supplementary Information).

Ionic conductivity measurements were evaluated as a function of salt concentration for P(EO-EPI)84:16 polymer electrolyte prepared with the plasticizer PEG-diB. The plasticized polymer electrolyte films (thickness of *ca.* 100 μm) were obtained by casting the electrolyte solutions onto a Teflon disk, under saturated atmosphere conditions. Afterwards, the films were detached from the Teflon by dipping into liquid nitrogen, and further dried under vacuum for 144 h. Conductivity measurements were carried out in a MBraun dry box (humidity < 10^{-4}%, under an argon atmosphere). The films were fixed between two mirror-polished stainless steel disc shaped electrodes (diameter = 12 mm) and the conductivity values were calculated from the data obtained by EIS, using an Eco-Chemie Autolab PGSTAT 12 with FRA module coupled to a computer in the frequency range of 10^{-6} to 10 Hz and amplitude of 10 mV applied to 0 V.

2.5. TiO_2 nanotube dye-sensitized solar cell assembly and characterization

DSSC were assembled using glass-FTO (Hartford glass, Rs ≤ 10 Ω cm^{-2}) and glass-ITO (Delta Technologies, Rs ≤ 30 Ω m^{-2}) electrodes as materials for the photoelectrodes and the counter-electrodes (CE), respectively. Thin platinum CE films (400 Å) were prepared by sputtering onto glass-ITO electrodes. For preparation of the photoelectrodes, a small aliquot of TiO_2 nanotube suspension was spread using a glass rod onto the glass-FTO electrodes with adhesive tape as spacer. The electrodes were heated at 450 °C for 30 min, cooled to ∼80 °C and then immersed in a 1.5×10^{-4} mol L^{-1} solution of the sensitizer dye *cis*-bis(4,4′-dicarboxy-2,2′-bipyridine)-bis(isothiocyanato)ruthenium(II) [$RuL_2(NCS)_2$] (Ruthenium-535, Solaronix) in absolute ethanol for 16 h. After that, the electrodes were rinsed with ethanol and dried. The polymer electrolyte was deposited by casting over the electrodes, previously placed on a hot plate at 60 °C to remove the solvent (acetone). Pressing the CE against the sensitized electrode coated with the polymer electrolyte finalized the assembly of the DSSC. An adhesive tape was placed between the two electrodes, in order to control electrolyte film thickness and to avoid short-circuiting of the cell. All devices were placed in a desiccator with P_2O_5 for 2 h to remove moisture. For comparison, TiO_2 nanotube DSSC were also assembled using a liquid electrolyte (0.5 mol L^{-1} *t*-butylpyridine, 0.6 mol L^{-1} tetrabutyl ammonium iodide, 0.1 mol L^{-1} LiI, 0.1 mol L^{-1} I_2 in 10 mL methoxyproprionitrile). A PVC film was placed in between the two electrodes to avoid short circuiting and electrolyte leakage. A clamp kept the assembly together. For the tests described in this communication, no further sealing was necessary. All solar cells assembled in this work had an active area of 0.3 cm^2.

The absorbance spectra of the TiO_2 nanoparticle and TiO_2 nanotube films covered with the ruthenium dye were measured in the reflectance mode using a spectrophotometer Guide Wave model 260.

The DSSC devices were characterized on an optical bench using an Oriel Xe(Hg) 250 W lamp, lenses, water and cut-off filters to avoid IR and UV radiation, respectively. The light intensity was measured with a Newport Optical Power Meter. Current–potential curves (*I–V* curves) were obtained by linear sweep voltammetry at 1 mV s^{-1} using the Eco Chimie-Autolab PGSTAT 12 potentiostat.

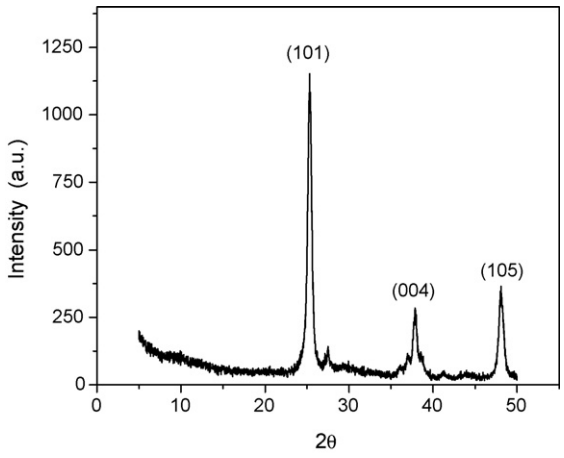

Fig. 1. XRD pattern of the TiO_2 nanotubes after calcination at 450 °C for 30 min.

3. Results and discussion

3.1. Morphology of the titania nanotubes

There is a controversy in the literature about whether the nanotubular structures formed by the hydrothermal treatment followed by HCl washing are TiO_2 or titanate ($H_2Ti_3O_7$) [41–45]. Among the controversies on composition and formation mechanism, different morphologies, such as nanorods, nanotubes, nanofibers and nanobelts, have been reported with some apparently similar hydrothermal processes. Kasuga et al. have speculated on the mechanism of TiO_2 nanotube formation and, according to their report, the titania nanotubes are formed during the washing with HCl [35]. In our experiment, we added a further step, introducing a calcination step at 450 °C for 30 min after the hydrothermal process. The XRD pattern (Fig. 1) of the solid obtained after calcination indicates that the crystalline phase formed is predominantly anatase TiO_2 with a minimal content of rutile phase (indicated by a peak at 27.5°). The lack of a peak at $2\theta \sim 10°$ assigned to titanate suggests that this material can be an intermediate but not a final product.

The Brunauer–Emmett–Teller (BET) specific surface area of the TiO_2 nanotubes was 200 $m^2\,g^{-1}$. This value is much higher in comparison to TiO_2 nanoparticles of ~50 $m^2\,g^{-1}$ (Degussa, P25).

SEM and TEM analyses were carried out in the dried solid after centrifugation and washing processes. From the SEM image (see Supplementary Information), a structure with fibrous-like material, displaying a very large surface area can be found everywhere. By TEM analysis, we verify that this material is composed by needle-shaped structures and sheets (Fig. 2A).

The contrast pattern suggests that the needle-shaped structures are in fact nanotubes as can be clearly seen in Fig. 2B and C. Indeed, closed TiO_2 nanotubules of ~3 nm of diameter are seen in Fig. 2B, visualized by the characteristic image contrast seen in the border of the tubes. Fig. 1C shows three nanostructures that resemble belts, which are probably the walls of open nanotubes. The patterns seen in the TEM images indicate these nanostructures are composed by single wall TiO_2 nanotubes with an internal diameter of ~3 nm, which is coincident with the value obtained by Wu et al. [38]. From both SEM and TEM images, we verify that our material exhibits a large distribution of lengths of TiO_2 nanostructures. Nanosheets with transversal and longitudinal lengths of up ~100 nm and 1 μm, respectively, are observed. This result is quite different from that observed by Kasuga et al. [34], where nanotubes of ~100 nm and diameter of 8 nm were produced. This can be possibly related to the long period for the hydrothermal treatment used in our procedure (the gel was kept in the autoclave for 48 h against 20 h in Kasuga's method) giving rise to this wide range of size distributions and shape.

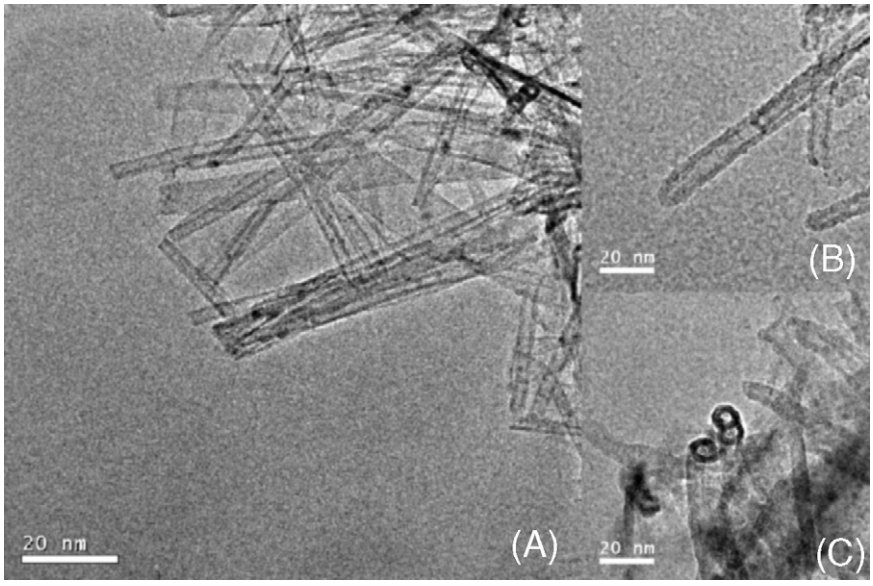

Fig. 2. TEM images of the TiO_2 nanotubes at different magnifications.

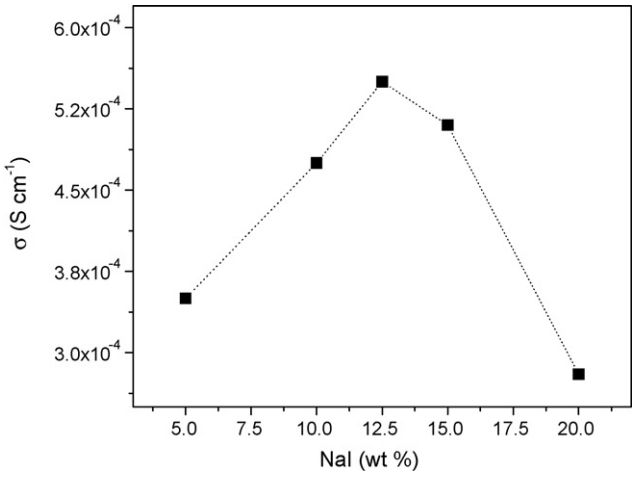

Fig. 3. Variation of the ionic conductivity of the plasticized polymer electrolyte P(EO-EPI)84:16/PEG-diB as a function of NaI concentration (28 ± 1 °C, $[H_2O] < 0.0001\%$).

3.2. Plasticized polymer electrolyte characterization

The ionic conductivity was calculated from the value of the bulk electrolyte resistance obtained in the complex impedance diagram. The ionic conductivities of P(EO-EPI)84:16/PEG-diB/NaI/I_2 samples (28 ± 1 °C, $[H_2O] < 0.0001\%$), with different salt concentrations, are shown in Fig. 3. It can be seen that the increase in salt concentration leads to an increase in the ionic conductivity (σ) of the plasticized polymer electrolyte up to 12.5 wt% NaI where the maximum value of 5.5×10^{-4} S cm^{-1} was obtained. A further increase in the NaI concentration produces a decrease in the ionic conductivity due to the formation of ion pairing and crosslinking sites that hinder the segmental motion of the polymeric chains [46]. The maximum value of ionic conductivity obtained is one order of magnitude higher than that of the polymer electrolyte without plasticizer [11,47,48]. The introduction of PEG-diB in the copolymer matrix also allows the dissolution of a higher amount of salt. Up to 15 wt% NaI, the ionic conductivity remains on the order of 10^{-4} S cm^{-1}. It is important to emphasize that these measurements were made under a strictly controlled low-humidity atmosphere since the presence of moisture affects the ionic conductivity [49].

The thermal behavior obtained by DSC and TGA analyses for P(EO-EPI)84:16/PEG-diB/NaI/I_2 samples with 5, 12.5 and 20 wt% NaI are discussed in Supplementary Information.

3.3. Titania nanotubes dye-sensitized solar cells assembly and characterization

The current–potential curves (*I–V*) obtained under different light intensities for a DSSC assembled with P(EO-EPI)84:16/PEG-diB + 12.5% NaI (1.25% I_2) and TiO_2 nanotubes are presented in Fig. 4. The electrical parameters are summarized in Table 1. For comparison, a DSSC composed of standard titania nanoparticles (Degussa P-25) was also assembled. It is important to emphasize that, comparison between a nanoparticulated and a nanotube film is not straightforward due to several parameters involved. Thus, we conducted our experiments by choosing films with the same thickness.

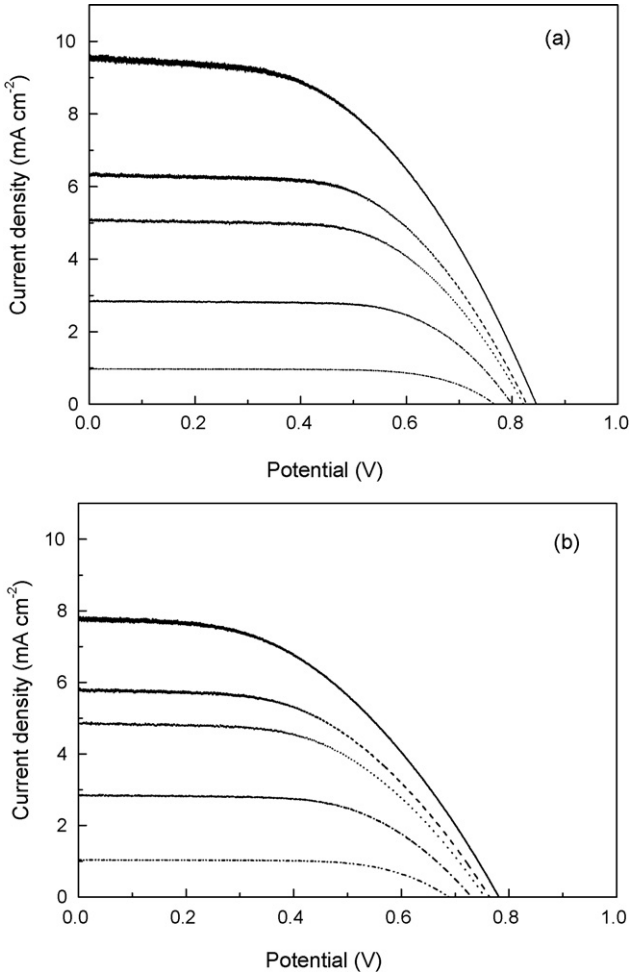

Fig. 4. Comparison of the current–potential curves obtained under different light intensities for the TiO_2 dye-sensitized solar cell assembled with the plasticized polymer electrolyte P(EO-EPI)84:16/PEG-diB + 12 wt% NaI/I_2: (a) device with TiO_2 nanotube film and (b) device with nanoparticulated film.

During DSSC characterization, we observed that the introduction of a thin layer of TiO_2 nanoparticulated film prior deposition of TiO_2 nanotubes layer was necessary to improve the electrical parameters as well as the adhesion of the nanotubes onto the FTO electrode. It is expected that the contact

Table 1
Comparison of the electrical characteristics of the dye-sensitized solar cells investigated in this work

I_{RR} (mW cm^{-2})	I_{SC} (mA cm^{-2})	V_{OC} (V)	FF (%)	η (%)
DSSC assembled with TiO_2 nanotubes and plasticized polymer electrolyte				
100	9.63	0.846	49	4.03
9	0.97	0.767	71	5.91
DSSC assembled with TiO_2 nanoparticles and plasticized polymer electrolyte				
100	7.75	0.781	47	2.84
9	1.04	0.688	66	5.28
DSSC assembled with TiO_2 nanotubes and liquid electrolyte				
100	12.47	0.829	55	5.64
9	1.11	0.743	70	6.66

between the nanotube layer and the glass substrate is poor due to their morphologies (long and disordered arrays of nanotubes) which may leave more free-contact space on the surface of glass, increasing the ohmic loss and the cell's dark current [22]. The titania films in both cases had the same thickness (∼12 μm). For the bilayer DSSC device, the titania film comprises 6 μm of nanoparticles and 6 μm of nanotubes.

The DSSC assembled with TiO_2 nanotubes presented much higher values of short-circuit current (I_{SC}), open circuit potential (V_{OC}), fill factor (FF) and overall conversion efficiency (η) in comparison to the cell assembled with titania nanoparticles (same film thickness of 12 μm). For the DSSC assembled with titania nanotubes, when the irradiation intensity was increased from 9 to 100 mW cm^{-2}, I_{SC} changed from 0.97 to 9.63 mA cm^{-2} with a slight increase in the V_{OC} from 0.767 to 0.846 V. In contrast the values of FF and η decreased when increasing the light intensity as expected for this type of solar cell. We can assign the drastic increase in the current density for the DSSC with TiO_2 nanotubes, in comparison to the cell assembled with titania nanoparticles as a result of two important properties derived from one-dimensional electrodes: (i) A much higher surface area which allows more sensitizer dye to be chemically anchored in the electrode and, as a consequence, the light harvesting is drastically improved. We measured the absorption spectra of the sensitized TiO_2 films by UV–vis–IR diffuse reflectance spectroscopy (Fig. 5). The data resembles the electronic absorption spectra of the ruthenium dye adsorbed in the titania films. In fact, the absorbance intensity measured for the TiO_2 sensitized nanotubes is about 3.5 times higher than the film containing sensitized titania nanoparticles (for the same film thickness). This data is found to be consistent with the amount of dye absorbed in the film formed by TiO_2 nanotubes [22,27]. (ii) Better penetration of the plasticized polymer electrolyte through the film, as a consequence of the open structure of the TiO_2 nanotubes shown by the images in Fig. 2. One of the relevant issues in DSSC using polymers is that there is no guarantee that all voids in the semiconducting film are completely filled by the polymer electrolyte because of its high molecular weight and low diffusion. As a consequence, charge recombination plays an effective role in the TiO_2/dye interface, competing successfully with the dye regeneration reaction.

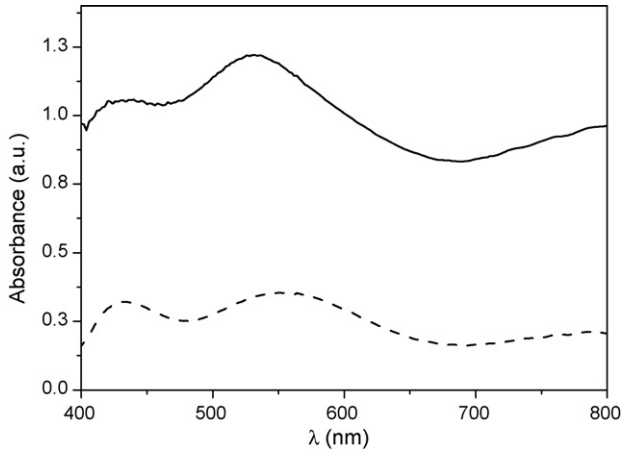

Fig. 5. UV–vis reflectance spectra of the TiO_2 films (12 μm) sensitized with Ruthenium-535 dye: TiO_2 nanotube/dye film (full line) and TiO_2 nanoparticulated/dye film (dashed line).

Thus, the morphology of the nanotube film creates an ample ion path for fast ionic motion from the bulk to the inner parts of the film. Although we did not measure the iodide diffusion coefficient in such network, this is expected to be higher when the TiO_2 nanotube structure is preferred. This effect can be evidenced by the increase in the fill factor and open-circuit voltage when the nanotubes are employed.

We cannot discard, however, the influence of the nanotube structure in the electronic transport. The use of this one-dimensional structure permits a high rate of electron transfer through the TiO_2 nanotubes, by decreasing the number of contact barriers between each particle [21,22,39,50]. In fact, Ohsaki et al. have evaluated the electron transport properties of these nanotubes. According to their results, TiO_2 nanotube electrodes have a longer electron lifetime and diffusion length than the electrodes made of P25 [39]. It is difficult to evaluate which parameters dominate in such a complex system. Particularly, in our study, and considering the character of the ionic transport medium (polymer), we believe that the gain in the performance of our solar cell is much more closely related to an increase in light absorption and to a better ionic diffusion, when replacing the nanoparticles by titania nanotube films.

The value for the overall efficiency at 100 mW cm^{-2} obtained with the TiO_2 nanotube DSSC is impressive. In general, when replacing the liquid electrolyte by a polymer one, the efficiency is drastically reduced at high illumination when the demands for a much more efficient ionic transport are required in order to regenerate all the photogenerated dye cations. Here, replacing the titania nanoparticles by titania nanotubes the overall efficiency reaches 4.03% for a DSSC assembled with a polymer electrolyte. It is an indication that, indeed, the combination of a one-dimensional electrode with plasticized polymer electrolytes can be an interesting alternative to push the efficiency up to values comparable to DSSC assembled with liquid electrolytes. For comparison, Table 1 also exhibits the electrical characteristics for a cell employing a liquid electrolyte and TiO_2 nanotubes. The overall efficiencies for both devices are very close, reaching 4.03 and 5.64% for the polymer and liquid electrolyte solar cells, respectively. Fig. 5 shows the short-circuit current dependence on light intensity (I_L) for both devices. I_{SC} increases linearly with light intensity and is higher for the devices using the liquid electrolyte. The I_{SC} dependence of light intensity follows a power law $I_{SC} \sim I_L^{\alpha}$. The exponent was found to be 0.94 and 1.0 for DSSC using polymer and liquid, respectively. The deviation from linearity at high light intensity levels observed for the DSSC assembled with the plasticized polymer electrolyte is a consequence of the reduced ionic mobility in the polymer medium. This data is in agreement with the better performance exhibited by the solar cells using liquid electrolyte. However, the proximity in the electrical parameters and the high efficiency at 100 mW cm^{-2} obtained when combining titania nanotubes and polymer electrolyte are remarkable when considering all the gains obtained

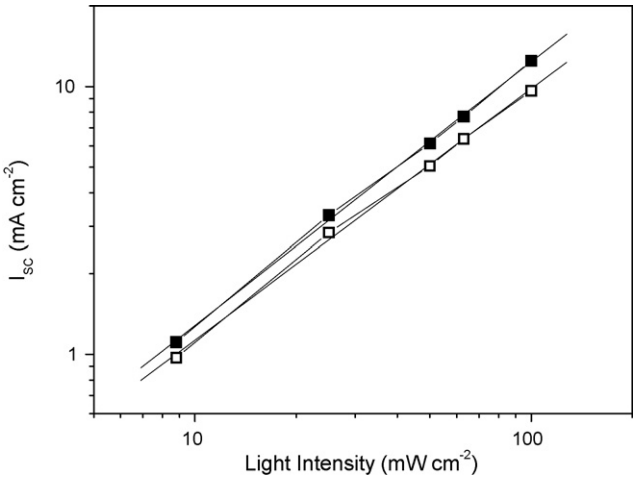

Fig. 6. Dependence of the photocurrent on light intensity for the TiO_2 nanotube DSSC cells assembled with liquid electrolyte (full square) and plasticized polymer electrolyte (open square).

(easy assembly and stability) when replacing the liquid by a polymer electrolyte, at a minimum cost in efficiency [51,52] (Fig. 6).

4. Conclusions

DSSC combining TiO_2 nanotubes and a plasticized polymer electrolyte have shown to be a promising alternative for assembling solar cells devices with good performance and easy assembling. The titania nanotubes prepared by a very simple and straightforward sol–gel method described in the literature present a suitable structure for depositing the polymer electrolyte film. The high surface area allows more ruthenium dyes to be anchored in the oxide surface and creates an ample ion path for fast ionic motion from the bulk to the inner parts of the film. The drastic increase in the current density observed can be described as a combination of these two factors, although we cannot eliminate the influence of these one-dimensional electrodes in the fast electronic transport.

Solar cells assembled by combining the TiO_2 nanotubes and the plasticized polymer electrolyte exhibited an overall efficiency of 4.03% at 100 mW cm^{-2}, higher than the devices assembled solely with TiO_2 nanoparticles. The easy preparation of these electrolytes compared to others found in the literature, easy cell assembly, the possibility to optimize both titania nanotube film and the device make the approach described in this work an interesting alternative for more efficient solid-state DSSC.

Acknowledgments

The authors thank the Brazilian agency FAPESP for financial support (Process 2004/06031-6), Daiso Ltd. (Osaka, Japan) for supplying the polymer samples and Prof. Carol Collins for English revision. The electron microscopy work has been performed with the JSM-6330F and JEM-3010 ARP microscopes of the Laboratório de Microscopia Eletrônica, LNLS, Campinas.

Appendix A. Supplementary data

Supplementary data associated with this article can be found, in the online version, at doi:10.1016/j.jphotochem.2007.01.023.

References

[1] B. O'Reagan, M. Grätzel, Nature 353 (1991) 737–740.
[2] M. Grätzel, J. Photochem. Photobiol. A: Chem. 164 (2004) 3–14.
[3] Y. Tachibana, J.E. Moser, M. Grätzel, D.R. Klug, J.R. Durrant, J. Phys. Chem. B 100 (1996) 20056–20062.
[4] Y. Saito, N. Fukuri, R. Senadeera, T. Kitamura, Y. Wada, S. Yanagida, Electrochem. Commun. 6 (2004) 71–74.
[5] Q.-B. Meng, K. Takahashi, X.-T. Zhang, I. Sutanto, T.N. Rao, O. Sato, A. Fujishima, H. Watanabe, T. Nakamori, M. Urigami, Langmuir 19 (2003) 3572–3574.
[6] W. Kubo, T. Kitamura, K. Hanabusa, Y. Wada, S. Yanagida, Chem. Commun. (2002) 374–375.
[7] P. Wang, S.M. Zakeeruddin, P. Comte, I. Exnar, M. Grätzel, J. Am. Chem. Soc. 125 (2003) 1166–1167.
[8] P. Wang, S.M. Zakeeruddin, R. Humphry-Baker, M. Grätzel, Chem. Mater. 16 (2004) 2694–2696.
[9] A.F. Nogueira, J.R. Durrant, M.-A. De Paoli, Adv. Mater. 13 (2001) 826–830.
[10] S.A. Haque, E. Palomares, H.M. Upadhyaya, L. Otley, R.J. Potter, A.B. Holmes, J.R. Durrant, Chem. Commun. 24 (2003) 3008–3009.
[11] A.F. Nogueira, C. Longo, M.-A. De Paoli, Coord. Chem. Rev. 248 (2004) 1455–1468.
[12] P. Wang, S.M. Zakeeruddin, J.E. Moser, M.K. Nazeeruddin, T. Sekiguchi, M. Grätzel, Nat. Mater. 2 (2003) 402–407.
[13] E. Stathatos, P. Lianos, S.M. Zakeeruddin, P. Liska, M. Grätzel, Chem. Mater. 15 (2003) 1825–1829.
[14] N. Mohmeyer, P. Wang, H.W. Schmidt, S.M. Zakeeruddin, M. Grätzel, J. Mater. Chem. 14 (2004) 1905–1909.
[15] R. Komiya, L. Han, R. Yamanaka, A. Islam, T. Mitate, J. Photochem. Photobiol. A: Chem. 164 (2004) 123–128.
[16] A.F. Nogueira, N. Alonso-Vante, M.-A. De Paoli, Synth. Met. 105 (1999) 23–27.
[17] A. Solbrand, H. Lindstrom, H. Rensmo, A. Hagfeldt, S.-E. Lindiquist, J. Phys. Chem. 101 (1997) 2514–2518.
[18] S. Kambe, S. Nakade, T. Kitamura, Y. Wada, S. Yanagida, J. Phys. Chem. B 106 (2002) 2967–2972.
[19] L. Dloczik, O. Ileperuma, I. Lauermann, L.M. Peter, E. Ponomarev, G. Redmond, N.J. Shaw, I. Uhlendorf, J. Phys. Chem. B 101 (1997) 10281–10289.
[20] A.C. Fisher, L.M. Peter, E.A. Ponomarev, A.B. Walker, K.G.U. Wijayantha, J. Phys. Chem. B 104 (2000) 949–958.
[21] M. Adachi, Y. Murata, J. Takao, J. Jiu, M. Sakamoto, F. Wang, J. Am. Chem. Soc. 126 (2004) 14943–14950.
[22] J.T. Jiu, S. Isoda, F.M. Wang, M. Adachi, J. Phys. Chem. B 110 (2006) 2087–2092.
[23] W.U. Huynh, J.J. Dittmer, A.P. Alivasatos, Science 295 (2002) 2425–2427.
[24] T. Lindgren, H.L. Wang, N. Beermann, L. Vayssieres, A. Hagfeldt, S.E. Lindquist, Sol. Energy Mater. Solar Cells 71 (2002) 231–243.
[25] M. Law, L.E. Greene, J.C. Johsson, R. Saykally, P. Yang, Nat. Mater. 4 (2005) 455–459.
[26] P. Ravirajan, A.M. Peiró, M.K. Nazeeruddin, M. Grätzel, D.D.C. Bradley, J.R. Durrant, J. Nelson, J. Phys. Chem. B 110 (2006) 7635–7639.
[27] J.-H. Yoon, S.-R. Jang, R. Vittal, J. Lee, K.-J. Kim, J. Photochem. Photobiol. A: Chem. 180 (2006) 184–188.
[28] Y. Gao, M. Nagai, Langmuir 22 (2006) 3936–3940.
[29] E. Hosono, S. Fujihara, I. Honma, H. Zhou, Adv. Mater. 17 (2005) 2091–2094.
[30] B. Tan, Y. Wu, J. Phys. Chem. B 110 (2006) 15932–15938.
[31] S. Uchida, R. Chiba, M. Tomiha, N. Masaka, M. Shirai, Electrochemistry 70 (2002) 418–420.
[32] G.K. Mor, K. Shankar, M. Paulose, O.K. Varghese, C.A. Grimes, Nano Lett. 6 (2006) 215.

[33] B.B. Lakshmi, P.K. Dorhout, C.R. Martin, Chem. Mater. 9 (1997) 857–862.
[34] T. Kasuga, M. Hiramatsu, A. Hoson, T. Sekino, K. Niihara, Langmuir 14 (1998) 3160–3163.
[35] T. Kasuga, M. Hiramatsu, A. Hoson, T. Sekino, K. Niihara, Adv. Mater. 11 (1999) 1307–1311.
[36] X.Y. Zhang, L.D. Zhang, W. Chen, G.W. Meng, M.J. Zheng, L.X. Zhao, Chem. Mater. 13 (2001) 2511–2515.
[37] T. Peng, A. Hasegawa, J. Qiu, K. Hirao, Chem. Mater. 15 (2003) 2011–2016.
[38] J.-J. Wu, C.-C. Yu, J. Phys. Chem. B 108 (2004) 3377–3379.
[39] Y. Ohsaki, N. Masaki, T. Kitamura, Y. Wada, T. Okamoto, T. Sekino, K. Niihara, S. Yanagida, Phys. Chem. Chem. Phys. 7 (2005) 4157–4163.
[40] M. Wei, Y. Konish, H. Zhou, H. Sugihara, H. Arakawa, J. Electrochem. Soc. 153 (2006) A1232–A1236.
[41] G.H. Du, Q. Chen, R.C. Chen, Z.Y. Yuan, L.M. Peng, Appl. Phys. Lett. 79 (2001) 3702–3704.
[42] Q. Chen, G.H. Du, S. Zhang, L.M. Peng, Acta Crystallogr. B 58 (2002) 587–593.
[43] B.D. Yao, Y.F. Chan, X.Y. Zhang, W.F. Zhang, Z.Y. Yang, N. Wang, Appl. Phys. Lett. 82 (2003) 281–283.
[44] W.Z. Wang, O.K. Varghese, M. Paulose, C.A. Grimes, Q.L. Wang, E.C. Dickey, J. Mater. Res. 19 (2004) 417–422.
[45] D. Wu, J. Liu, X.N. Zhao, A.D. Li, Y.F. Chen, N.B. Ming, Chem. Mater. 18 (2006) 547–553.
[46] R.A. Robinson, R.H. Stokes, Electrolyte Solutions, Butterworths, 1959.
[47] A.F. Nogueira, M.A.S. Spinacé, W.A. Gazotti, E.M. Girotto, M.-A. De Paoli, Solid State Ionics 140 (2001) 327–335.
[48] V.C. Nogueira, C. Longo, A.F. Nogueira, M.A. Soto-Oviedo, M.-A. De Paoli, J. Photochem. Photobiol. A: Chem. 181 (2006) 226–232.
[49] A.E. Wolfenson, R.M. Torresi, T.J. Bonagamba, M.-A. De Paoli, H. Panepucci, J. Phys. Chem. B 101 (1997) 3469–3473.
[50] M.S. Dresselhaus, Y.M. Linb, O. Rabinc, A. Jorioa, A.G. Souza Filho, M.A. Pimenta, R. Saitof, G.G. Samsonidzeb, G. Dresselhaus, Mater. Sci. Eng. C 23 (2003) 129–140.
[51] M. Durr, G. Kron, J.H. Werner, A. Yasuda, G. Nelles, J. Chem. Phys. 121 (2004) 11374–11378.
[52] W. Kubo, K. Murakoshi, T. Kitamura, S. Yoshida, M. Haruki, K. Hanabusa, H. Shirai, Y. Wada, S. Yanagida, J. Phys. Chem. B 51 (2001) 12809–12815.